Volume 1 | Number 1 | Jan 2013 | Pages 1–100

PCCP

Physical Chemistry Chemical Physics
www.rsc.org/pccp

ROYAL SOCIETY OF CHEMISTRY

ROYAL SOCIETY OF CHEMISTRY

www.rsc.org/pccp

Theoretical study of the OH-initiated atmospheric oxidation mechanism

of perfluoro methyl vinyl ether, CF$_3$OCF=CF$_2$

L. Vereecken,[a,*] J. N. Crowley,[a] D. Amedro[a,b]

[a] Max Planck Institute for Chemistry, Atmospheric Sciences, Hahn-Meitner-Weg 1, Mainz, Germany

[b] Division of Chemistry and Chemical Engineering, California Institute of Technology, Pasadena, CA, U.S.A.

* Email: Luc.Vereecken@mpic.de

Abstract

Product formation in the reaction of perfluorinated methyl vinyl ether, CF$_3$OCF=CF$_2$, with OH radicals is studied theoretically using the M06-2X/aug-cc-pVTZ and CCSD(T) levels of theory. The stable end-products in an oxidative atmosphere are predicted to be perfluorinated methyl formate, CF$_3$OCFO, and fluorinated glycolaldehyde, CFOCF$_2$OH, both with CF$_2$O as coproduct. The prediction of glycolaldehyde as a product contrasts with experimental data, which found perfluoro glyoxal, CFOCFO, instead. The most likely explanation for this apparent disagreement is conversion of CFOCF$_2$OH to CFOCFO, e.g. by multiple catalytic agents present in the reaction mixture, wall reactions, and/or photolysis. The formation routes for the glyoxal product proposed in earlier work appear unlikely, and are not supported by theoretical or related experimental work.

Table of Content Graphic
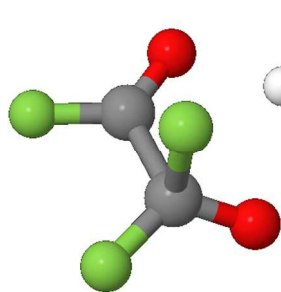
The fluorinated product glycolaldehyde can be catalytically converted to glyoxal + HF by H$_2$O.

1. Introduction

In applications such as refrigeration systems or electronics cleaning, fluorinated organic compounds are used as possible replacements for chloro- or bromo-substituted compounds, to avoid the adverse effects these latter compounds can have on the stratospheric ozone layer.[1–3] Fluorinated organic compounds are also extensively used in the production of plastics, elastomers and membranes, owing to their specific thermal and chemical properties.[4,5] Perfluoro methyl vinyl ether (PMVE), $CF_3OCF=CF_2$ (classified as hydrofluoroether HFE-216), can be used in the production of perfluoroalkoxy polymers (PFA),[4] as well as in plasma etching processes.[6,7] Evaporation and spills during the use of PMVE result in its release to the atmosphere.

The dominant degradation channel for PMVE in the atmosphere is the reaction with OH radicals, which is initiated by addition on the double bond. The rate coefficient of this reaction was measured at 3×10^{-12} cm^3 molecule^{-1} s^{-1} at 296 K.[8–10] A positive temperature dependence was reported by Li et al.,[9] with an activation energy of 1.7 kcal mol^{-1}, while Tokuhashi et al.[10] report a negative temperature dependence, with an activation energy of -0.63 kcal mol^{-1}. In their mass spectrometric study at 1 Torr He as a bath gas, Li et al.[9] observed the formation of HF and $^\bullet$CFO radicals as products. The end-product study of Mashino et al.[8] at 700 and 10 Torr of air indicated formation of CF_2O, CF_3OCFO, and CFOCFO, with yields of 90 ± 5, 53 ± 4, and 40 ± 5 %, respectively, at 700 Torr, and 104 ± 6, 8 ± 2, and 69 ± 8 % at 10 Torr. Mashino et al.[8] do not report observation of HF in their infrared spectra, which may either be a result of its non-formation in air at pressures above 10 Torr, lack of detection sensitivity, or a loss process. The products formed in both these studies,[9,8] and the observed product yield pressure dependence were rationalized by prompt HF elimination from the initial adduct formed by addition of OH to the $=CF_2$ carbon, as shown in Figure 1 (bold arrows), in competition with collisional stabilisation of the chemically activated adduct.

2

Recent theoretical work on the mechanism of the highly similar OH-initiated oxidation of perfluoro propyl vinyl ether (PPVE), however, did not predict formation of HF and CFOCFO.[11] To our knowledge, the $CF_3OCF=CF_2$ + OH reaction has not been studied theoretically before. We present a quantum chemical analysis of the atmospheric degradation pathway of this compound initiated by OH, use simplified RRKM master equation calculations to examine the most likely products, and compare these results to the available experimental product data.

2. Theoretical methodology

Critical intermediates and transition states for reactions involved in the atmospheric oxidation of PMVE were investigated using M06-2X/aug-cc-pVTZ,[12,13] where zero-point vibrational energy was scaled by 0.971.[14,15] The relative energies are estimated to carry uncertainties of up to 4 kcal mol^{-1} at this level of theory,[12,16,17] making absolute predictions of the rate coefficients less reliable. However, the relative contribution of competing reactions can be determined sufficiently accurate; more specifically, the large differences (> 10 kcal mol^{-1}) in the calculated barrier heights and/or reaction energies provides a sufficiently accurate, quantitative view to correctly deduce the dominant reaction pathway. The supporting information tabulates single point CCSD(T)/6-311++G(d,p), CCSD(T)/aug-cc-pVDZ, and some CCSD(T)-F12a/aug-cc-pVDZ calculations, for comparison against the M06-2X results used here. For the most critical reaction pathways, we find average energy differences of the order of 2 kcal mol^{-1} only; variation of the energetics by this amount does not affect the results in this paper. All quantum chemical calculations were performed using Gaussian-09.[18]

Simplified canonical transition state theory (CTST) calculations for the rate coefficient of the title reaction were performed to obtain information on its temperature dependence, and on the relative contribution of the two adducts. These CTST results are discussed in the supporting information only,

3

as such calculations are critically sensitive to the absolute barrier heights, and the absolute rate coefficient values carry a rather large uncertainty.

To assess the impact of chemical activation on the fate of the initial PMVE-OH adducts, we performed RRKM master equation calculations, implemented using the DCPD methodology[19] that gives information on the energy-specific fate of the molecule. The molecule is modelled as a rigid rotor with harmonic oscillators, except for the degrees of freedom for internal rotation (up to 4 modes). These are described as a symmetric 1-dimensional separable hindered internal rotor, calculating the quantum energy states as described by Barker and Shovlin[20] and Troe[21] i.e. as harmonic oscillators below the hindrance potential barrier, and as a free rotor above that barrier. Reduced moments of inertia are obtained following the method by Kilpatrick and Pitzer.[22] Lennard-Jones collision parameters of the adducts are estimated as $\sigma = 6.5$ Å, $\varepsilon = 360$ K, with an average $\Delta E_{down} = \sim300$ cm^{-1} in the exponential-down energy transfer model, with air as a bath gas; some variations of ΔE_{down} were examined (see below). The level of theory employed here is intended mainly to provide a semi-quantitative view of the reaction kinetics. E.g. the treatment of internal rotors is rudimentary; at the same time, it does reflect the change in state density upon gain or loss of an internal rotor in the TS relative to the reactant, which is the most critical aspect, and improving the internal rotor model will have a limited impact due to cancellation of error. The current theoretical analysis should only be used as a guide to establish the most likely atmospheric oxidation scheme of the PMVE molecule, rather than as a source of accurate absolute values.

3. Oxidation mechanism

The degradation mechanism is depicted in Figure 2 for the dominant adduct channel where OH adds to the outer carbon of the C=C double bond, and Figure 3 for the minor adduct channel with

OH adding to the double bond inner C-atom. The full set of quantum chemical data is available in the supporting information, which also includes Figures SI-1 and SI-2 showing additional reaction pathways.

The alkene + OH reactions proceed through a pre-reactive complex, and the reaction is kinetically controlled by two sets of reaction transition states, with the outer transition states governing the initial complex formation, and the inner transition states relate to the addition process on the double bond. We found pre-reactive complexes at up to 3.2 kcal mol^{-1} below the reactants, while the inner addition TS were at -2.1 and -1.5 kcal mol^{-1} below the reactants, for formation of $CF_3OC^{\bullet}F-CF_2OH$ and $CF_3OCF(OH)-C^{\bullet}F_2$, respectively. The pre-reactive complexes show H-bonding between the OH hydrogen and the F- or O-atoms, in contrast to traditional, non-fluorinated alkene + OH reactions where the pre-reactive complex shows a T-shape bonding the OH hydrogen to the π-bond,. This critical difference is related to the electron-withdrawing effect of the fluorine atoms from the π-bond. The submerged barriers for addition support a negative temperature dependence of the rate coefficient (see supporting information), in agreement with Tokuhashi et al.;[10] recent experimental work by Amedro et al.[11] on the analogous perfluoro propyl vinyl ether likewise found a negative temperature dependence. Note that rate coefficient calculations with higher addition barriers leads to k(T) predictions that become incompatible with the experimental data(see supporting information); e.g. an increase of the addition barrier by 2 kcal mol^{-1} yields rate coefficients over an order of magnitude below the available experimental data.

The addition reaction is exothermic by 54 and 52 kcal mol^{-1}, for addition on the outer or the inner carbon respectively. The formation of these β-hydroxy-alkyl radicals is in agreement with literature data on other fluorinated alkenes, and is significantly more exothermic than in analogous non-fluorinated compounds, e.g. for $CH_3OCH=CH_2$ + OH the exothermicity is only ~32 kcal mol^{-1}. It is

also significantly more exothermic than Cl-atom addition on PMVE, for which we calculate an energy well depth of ~27 kcal mol^{-1}.

For the dominant adduct, $CF_3OC^{\bullet}F-CF_2OH$, we have examined 8 possible unimolecular reaction channels (see Figure SI-1). F-atom loss forming $CF_3OCF=CFOH$ was found to be endothermic by 65 kcal mol^{-1} (relative to the adduct), the 1,5-HF-elimination channel with fragmentation has a barrier of 62 kcal mol^{-1}, a 1,2-F-migration forming $CF_3OCF_2-C^{\bullet}FOH$ shows a barrier of 36 kcal mol^{-1}, a 1,3-H-migration channel forming $CF_3OCFH-CF_2O^{\bullet}$ has a barrier of 39 kcal mol^{-1}, and formation of epoxides after 1,4- and 1,5-HF elimination is endothermic by 34 kcal mol^{-1} and 40 kcal mol^{-1}, respectively. This leaves the 1,2-HF elimination forming $CF_3OC^{\bullet}F-CFO$ (barrier 35 kcal mol^{-1}), and dissociation forming $^{\bullet}CF_3$ and $CFO-CF_2OH$ (barrier 24 kcal mol^{-1}), as the energetically lowest two channels, as shown in Figure 2. The barrier for HF elimination is directly comparable to earlier theoretical work on fluorinated methanol.[23–28] For the experimental conditions of Mashino et al.,[8] the $^{\bullet}CF_3$ radical reacts with O_2 (present in concentrations of several Torr) and NO (several mTorr) to form $CF_3O^{\bullet}$, which reacts rapidly[8,3,29] with NO to form CF_2O. In atmospheric conditions, $CF_3O^{\bullet}$ reacts either with NOx or hydrocarbons, forming CF_2O or CF_3OH, respectively.[29–33]

We have also attempted to find roaming pathways for the $^{\bullet}CF_3$ moiety, but were unable to identify any; the channels examined always connected to a shallow complex of the relevant fragments and are as such not fundamentally different from secondary chemistry, other than with respect to the internal energy content of the complex. The abstraction of an F-atom by the $^{\bullet}CF_3$ radical from its $CFOCF_2OH$ coproduct, forming $CF_4 + CFO-C^{\bullet}FOH$, could lead to glyoxal after the reaction with O_2, but has a high barrier 47 kcal mol^{-1}. Abstraction of the aldehyde group F-atom has an even higher barrier of 55 kcal mol^{-1}, as it does not form a vinoxy-stabilized radical. H-abstraction by $^{\bullet}CF_3$, forming $HCF_3 + CFO-CF_2O^{\bullet}$, has a barrier of 28 kcal mol^{-1}. Decomposition of this latter radical by C–C bond

scission has a barrier of only 1 kcal mol^{-1}, such that formation of glyoxal via F-abstraction by NO, similarly exothermic as the $CF_3O^{\bullet}$ + NO loss process, will not be able to compete. While the F- or H-abstraction channels by $^{\bullet}CF_3$ may have roaming equivalents we have not discovered, it appears unlikely that these channels are competitive against the $^{\bullet}CF_3$ loss. Roaming reactions usually have a fairly small contributions, and glycolaldehyde would remain the primary product of the prompt decomposition. The energies obtained for the above reactions are again in good agreement with analogous reactions described in the literature.[34–37,25]

The minor adduct, $CF_3OCF(OH)–C^{\bullet}F_2$, has access to similar decomposition routes (see Figure 3, see Figure SI-2); the main exception is that CF_3 elimination is not accessible, as it leads to a high-energy diradical rather than a stable carbonyl compound. Its lowest accessible unimolecular decomposition channel is HF loss, with a barrier of 39 kcal mol^{-1}.

In the atmosphere, and in the experiments by Mashino et al.[8], the adduct, $CF_3OC^{\bullet}F–CF_2OH$, can also be collisionally stabilized, and react with O_2, (see Figure 2) forming the $CF_3OCF(OO^{\bullet})–CF_2OH$ peroxy radical. We were unable to find easily accessible isomerisation channels for this peroxy radical, e.g. H-migration forming a hydroperoxide alkoxy radical is endothermic by 23 kcal mol^{-1}, so we assume the RO_2 reacts primarily with either NO or RO_2 to form the oxyradical $CF_3OCF(O^{\bullet})–CF_2OH$. Fluorinated RO_2 + NO reactions have low nitrate yields,[38] and these were not observed by Mashino et al.[8] The oxyradical has three accessible reaction channels: (*i*) loss of an F-atom with a barrier of 26 kcal mol^{-1}, forming $CF_3OC(=O)CF_2OH$ + F, (*ii*) breaking of the O–C bond with a barrier of 19 kcal mol^{-1}, forming a $CF_3O^{\bullet}$ radical and $CFOCF_2OH$ (fluorinated glycolaldehyde), and (*iii*) breaking the C–C bond with a barrier ≤ 1 kcal mol^{-1}, forming CF_3OCFO formate and the $^{\bullet}CF_2OH$ radical. This latter radical is expected to quickly react with O_2 forming F_2CO and HO_2. The low decomposition barrier for C–C bond breaking compared to the other pathways is in agreement with

observations and calculations for non-fluorinated alkoxy radials.[39–41] F-abstraction by O_2 atoms,

forming FO_2 radicals, is endothermic by over 20 kcal mol^{-1}.

The fate of the stabilized minor adduct, $CF_3OCF(OH)–C^•F_2$, is analogous, with addition of O_2,

conversion to the alkoxy radical, and C–C bond scission as the dominant channels, forming CF_3OCFO,

F_2CO and HO_2, similar to the main adduct (see Figure 3).

RRKM master equation calculations on the fate of the chemically activated initial adducts,

$CF_3OC^•F–CF_2OH$ and $CF_3OCF(OH)–C^•F_2$, showed that only one unimolecular decomposition channel

is competitive against collisional stabilization, specifically the formation of $^•CF_3$ and $CFO–CF_2OH$

(glycolaldehyde) from the main adduct $CF_3OC^•F–CF_2OH$. While our calculations are not sufficiently

accurate for an *a priori* prediction of the prompt decomposition yield, the estimated collisional energy

transfer parameters we used, in conjunction with our simple model for internal rotation, is fully

compatible with a decomposition yield of 40%, i.e. the yield of the aldehyde product observed by

Mashino et al.[8] More critically, though, is that it was impossible to find a physically acceptable set of

parameters at 700 Torr that allows for a significant amount of HF elimination formation from the

adducts. Even when reducing the average energy transferred per collision by a factor of 100, i.e. ΔE_{down}

$= \sim 3$ cm^{-1}, and removing the $^•CF_3$ loss channel from the master equation, the HF yield remains less

than 1 %. The HF elimination channel barrier is significantly higher than the $^•CF_3$ dissociation channel,

and is furthermore entropically disfavoured owing to the loss of 1 internal degree of rotation. Even at

the nascent energies, then, the unimolecular rate coefficient for HF elimination is small compared to the

collision number, and even slow energy loss prevents HF elimination. In addition, the competition

between the $^•CF_3$ loss and HF elimination strongly favours formation the formation of $^•CF_3$ +

glycolaldehyde, by a factor of $\sim 10^4$. Even though our kinetic model is rather simple, and the underlying

quantum chemical calculations are not the highest level possible, it is clear that this latter channel will

be the dominant channel in chemically activated unimolecular reactions. Prompt decomposition of the fluorinated glycolaldehyde product has a significant energy barrier of 45 kcal mol^{-1} for HF formation; given the energy distribution after the CF$_3$ elimination over the degrees of freedom of the two fragments and their relative motion, no significant direct HF formation is predicted. RRKM master equation calculations for a pressure of 10 Torr predict near-complete prompt decomposition of the main adduct through the $^\bullet$CF$_3$ + glycolaldehyde channel, while the minor adduct gets collisionally stabilized and reacts to methyl formate, as at higher pressures. Assuming a canonical energy distribution over the two addition TS (see supporting information), we find an 85:15 relative yield between the main and minor adducts at the 10 Torr, 296 K conditions of Mashino et al.[8] Their observed 69±8% yield of glyoxal in these conditions thus seems to reflect the contribution of OH addition on the outer carbon, followed by prompt $^\bullet$CF$_3$ loss from this adduct. Only 8±2% of methyl formate was observed; however, the experimental reaction mass balance is not fully closed, such that this number is hard to interpret as a measure of the contribution of the minor adduct. Finally, for the Cl-initiated oxidation of PMVE, our RRKM calculations predict negligible prompt decomposition owing to the significantly lower addition exothermicity of only 27 kcal mol^{-1}. This is in full agreement with Mashino et al.[8] who observed 100% yield of CF$_3$OCFO + CF$_2$O from this reaction.

The IR product spectrum obtained by Mashino et al.[8] shows a feature peak that matches closely to the absorption of the carbonyl moiety in fluorinated glyoxal. We have therefore examined some additional pathways that could lead to glyoxal (see Figure 1). Forming CFOCFO from the products of the lowest energy channels of the main adduct requires surmounting very high barriers: 30 kcal mol^{-1} for $^\bullet$CF$_3$ loss from CF$_3$OC$^\bullet$F–CFO, and 45 kcal mol^{-1} for 1,2-HF elimination from O=CF–CF$_2$OH. Formation of glyoxal from the O–C bond scission in the alkoxy radical is likewise not competitive against the C–C bond scission (see Figure 1). The calculations thus do not support the

glyoxal formation route proposed by Li et al.[9] and Mashino et al.[8] We have also examined some secondary chemistry, though an extensive quantum chemical investigation of all such reactions is outside the scope of this paper. F-abstraction by NO from closed-shell species such as $CFO\text{-}CF_2OH$ is strongly endothermic by 53 kcal mol^{-1} and can be neglected. As discussed higher, H- or F-atom abstraction by $^\bullet CF_3$ radicals from glycolaldehyde have high barriers, and are likewise non-competitive. Abstraction reactions by $CF_3O^\bullet$ radicals are expected to have slightly lower barriers than for $^\bullet CF_3$, but remain significantly too high to contribute. Analogous to CF_3OH chemistry, we surmise that HF-elimination from fluorinated glycolaldehyde could also be catalyzed by a number of compounds. As an example, we characterized the transition state for HF-elimination from fluorinated glyocolaldehyde catalyzed by H_2O:

$$CFOCF_2OH + H_2O \rightarrow CFOCFO + HF + H_2O$$
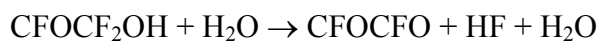
and found that the water molecule reduces the energy barrier to less than 15 kcal mol^{-1} relative to the free reactants, i.e. a reduction of 30 kcal mol^{-1} compared to the unimolecular decomposition barrier of 45 kcal mol^{-1}. Catalysis reactions for the decomposition of glycolaldehyde to glyoxal + HF are discussed in more detail below.

4. Discussion

The product distribution obtained above from theory-based data does not fully agree with the available experimental data. Both approaches agree on the ultimate formation of CF_3OCFO (perfluorinated methylformate) and CF_2O (perfluorinated formaldehyde), acting in competition with the chemically activated formation of a carbonyl compound with again CF_2O as its coproduct. The disagreement lies in the predicted carbonyl compound in this latter channel, where the experimental data points towards the formation of perfluorinated glyoxal, CFOCFO, after prompt HF elimination,

whereas the theory-based evidence supports formation of fluorinated glycolaldehyde, $CFOCF_2OH$,

after prompt $^\bullet CF_3$ loss. In our recent experimental and theoretical study[11] on perfluoro propyl vinyl

ether, $C_3F_7OCF=CF_2$, we also found no indications for HF elimination, or formation of perfluorinated

glyoxal formation, CFOCFO, with a large yield.

CFOCFO was not observed in the case of OH-initiated oxidation of hexafluoropropene,

$CF_3CF=CF_2$, at room temperature,[42,43] yielding CF_2O and CF_3OCFO as major products; this is

supported by a recent theoretical kinetic study by Saheb and Pourhaghighi,[34] and others.[35–37,44] The

ether functionality in $CF_3OCF=CF_2$ thus appears responsible for an additional product channel, yet the

proposed HF elimination route[9,8] is not expected to be dependent the presence or absence of the oxygen

atom.

In their mass spectrometric analysis of product formation at 1 Torr of He, Li et al.[9] observed

the formation of $^\bullet CFO$ radicals (m/z = 47), and of HF molecules (m/z = 20). These were hypothesized

as resulting from the HF loss route shown in Figure 1, followed by loss of $^\bullet CFO$ from the resulting

$CF_3OC^\bullet FCFO$ radical; this latter radical was not observed directly. CFO ions were also observed from

fragmentation of the $CF_3OCF=CF_2$ reactant, which suggests that sufficient energy is available in the

electron-impact ionisation stage to allow for complex ion rearrangements and fragmentation. Li et al.[9]

did not discuss the possibility that the observed HF and CFO fragments arose from fragmentation of

fluorinated glycolaldehyde, $CFOCF_2OH$. Mashino et al.[8] ruled out that HF arose via reaction of H-

atoms (used to form OH via reaction with added NO_2) with $CF_3OCF=CF_2$, but did not consider e.g.

reactions of H-atoms with the initial adducts. We note that formation of HF from $CF_3OC^\bullet F–CF_2OH$ +

$H^\bullet$ is exothermic by ~60 kcal mol^{-1}, but without knowledge of the relative concentrations of e.g. H and

NO_2 we cannot assess its impact.

The FTIR product measurement (1800 to 2000 cm^{-1}) by Mashino et al.[8] provides direct

evidence for formation of CF_2O, CF_3OCFO and CFOCFO. A possible, but unlikely explanation for the discrepancy between theory and experiment could be that the carbonyl stretch peaks of CFOCFO and $CFOCF_2OH$ are sufficiently similar to be virtually indistinguishable in the product spectrum; a reference IR spectrum of $CFOCF_2OH$ is not available. Exploratory calculations for the IR spectra at various levels of theory found differences of less than 15 cm^{-1} for the (an)harmonic carbonyl stretch peak positions, but are insufficient to conclude that the absorption band structure would strongly overlap. A direct experimental comparison of the peak position and branch shapes would be required to confirm this option.

Another possibility to reconcile theory with the experimental observations would be that glyoxal is formed in secondary chemistry, potentially induced or enhanced by the irradiation of the reaction mixture. Abstracting an F-atom from fluorinated glycolaldehyde, forming $CFOC^{\bullet}FOH$ radicals, would readily lead to glyoxal in the presense of O_2. H-abstraction, forming $CFOCF_2O^{\bullet}$ radicals, could likewise yield glyoxal if followed by F-abstraction by NO similar to the $CF_3O^{\bullet}$ + NO reaction (though it seems improbable that this can compete against dissociation to $^{\bullet}CFO + CF_2O$). However, our exploratory calculations discussed higher with abstraction agents present in the reaction mixture showed appreciable energy barriers, making these reactions unlikely. Catalytic HF elimination from CF_3OH, a simpler analogue of $CFOCF_2OH$, has been studied intensively theoretically,[28,23,25,45,26,24] and was found to be the key to understanding the rapid loss of CF_3OH in many experiments, on a time scale of minutes to hours, while other experiments found very long lifetimes.[46–50] The CF_3OH dissociation was found to be catalyzed by surfaces, by H_2O and $(H_2O)_2$, as well as by aqueous particles;[25,45,23] our characterization of an H_2O-catalysed HF-elimination from fluorinated glycolaldehyde with a barrier reduction of ~30 kcal mol^{-1} strongly suggests that $CFOCF_2OH$ behaves similar to CF_3OH in this respect. CF_3OH dissociation is also self-catalysed by other CF_3OH

molecules,[24] as well as by HF and $(HF)_2$ molecules,[28,24] which allows for an autocatalysis mechanism. Considering the mechanism for these reactions, other species such as carboxylic acids, hydroperoxides, HONO and HNO_3 are also potential catalysts. Finally, the presence of OH and HO_2 radicals can induce additional reductions in barrier height for water or HF complexes of CF_3OH.[25,26,24] All of these catalysts lower the barrier to formation of HF + CF_2O by tens of kcal mol^{-1}; if sufficient concentrations of catalysts are present, lifetimes of less than a minute[24] are predicted. It appears reasonable to assume that fluorinated glycolaldehyde, $CFOCF_2OH$, could undergo similar catalytic conversions, and the appropriate catalysts are known to have been present in the experiments referenced in this work. Insufficient information is available at this time to perform a modeling study, but a lower limit on the reaction rate coefficients can be derived from the dependence of the glyoxal yield as a function of $CF_3OCF=CF_2$ consumed, as measured by Mashino et al.[8] across 10 intervals within experiments taking 10 to 30 minutes. The observed linear dependence implies that the glycolaldehyde is converted near-completely to glyoxal within each product measurement interval of ≥ 1 min length, requiring a pseudo-first order conversion rate of the order of 0.05 s^{-1} or faster even during the first interval where product concentrations of appr. 0.15 mTorr are measured. A bimolecular catalysis reaction with a rate coefficient of $\sim 10^{-14}$ cm^3 molecule^{-1} s^{-1}, which in turn implies a reaction barrier of ~ 4 kcal mol^{-1} or less, would then be sufficient to convert the glycolaldehyde to glyoxal sufficiently fast. Heterogeneous catalysis on the wall could make the conversion rate less- or independent of catalyst concentrations, but implies sufficiently fast mixing to allow most products contact with the reactor wall.

A third possibility is a photolysis process for the fluorinated glycolaldehyde, where the lowest decomposition channel leads to HF + perfluoroglyoxal, with a barrier of 45 kcal mol^{-1}, i.e. requiring a ~ 635 nm photon. Buszek and Francisco[25] characterized enhanced photochemical decomposition of CF_3OH+water complexes by overtone induced excitation, suggesting that again complexation with species present in the reaction mixture could enhance decomposition. Fluorinated aldehydes and

alcohols, however, are not known to have a large absorption cross section in the UV/VIS spectral region, and the 22 fluorescent blacklamps used by Mashino et al.[8] are probably insufficient to induce a complete photochemical conversion of fluoroglycolaldehyde to perfluoroglyoxal on a timescale of 10s of seconds.

Finally, we examine the possibility that the discrepancy is caused by a fundamental error in the theoretical calculations. To bring out glyoxal+HF formation as the dominant prompt decomposition channel, at least two features on the current potential energy surface (see Figure 1) need to be strongly biased. The barriers for HF loss in fluorinated hydroxy-substituted molecules has been studied extensively theoretically; for all comparable molecules, and across a variety of levels of theory,[23–26,28,35–37,45,51] the barrier was found to be comparable to or higher than the barriers we have derived here. The pathway proposed by Mashino et al.[8] furthermore requires an alkoxy radical decomposition in a way that is not supported by theory or experimental work on RO-substituted alkoxy radicals.[39,40] Experimental work on the $CF_3CF=CF_2$ + OH reaction,[42] which proceeds through highly comparable intermediates, did not show HF formation or formation of glyoxal. Theoretical work on this latter reaction[35–37,44,34] likewise did not predict appreciable HF loss at temperatures below 500K, in agreement with our master equation analysis. The appearance of a carbonyl product in $CF_3OCF=CF_2$ as opposed to $CF_3CF=CF_2$ thus suggests that specifically the ether functionality allows for a lower-lying decomposition channel, which we predict to be the $^\bullet CF_3$ loss. We can not exclude, despite our extensive efforts to find all pathways, that we were unable to find an alternative decomposition channel leading to HF and glyoxal, that is competitive against the $^\bullet CF_3$ loss; it is not clear by which mechanism that channel could proceed. Also, the kinetic methodology used here would break down if the energy distribution after addition of OH on $CF_3OCF=CF_2$ would be highly non-statistical, controlling the decomposition dynamics by favoring HF loss and glyoxal formation. We have no knowledge of any

evidence of such non-statistical behavior in OH-addition on (halogenated) alkenes.

5. Conclusions

We report a theoretical kinetic study of the product formation in the reaction of OH radicals with perfluorinated methyl vinyl ether (PMVE), and compare it against the available experimental data. We find submerged barriers for OH addition on the double bond, supporting a negative temperature dependence of the rate coefficient. The main products are predicted to be CF_3OCFO, perfluoro methylformate, and CF_2O, perfluoro formaldehyde. There is evidence of a significant yield, $\sim 40\%$ at 1 atm, of a second carbonyl product, which is theoretically predicted to be fluorinated glycolaldehyde, $CFOCF_2OH$, but which experimental data detects as perfluoro glyoxal, CFOCFO. The simplest way to bring both sets of data in agreement is when the infrared carbonyl stretch peak in both fluorinated glycolaldehyde and glyoxal would, serendipitously, have a highly similar position and shape such that they could not be distinguished in the IR spectra; no experimental reference spectrum of $CFOCF_2OH$ is available, to our knowledge. An alternative explanation is that the fluorinated glycolaldehyde is converted to perfluoro glyoxal + HF, under the catalytic influence of H_2O, HF, OH, HO_2, fluorinated glycolaldehyde itself, dimers of these catalysts, wall reactions, or by (catalyzed) photolysis. This conversion could not be proven due to a lack of data, but its potential is carried by the ample literature on the analogous catalyzed $CF_3OH \rightarrow CF_2O + HF$ decomposition. The formation pathway for glyoxal proposed in earlier work is not supported by theory, and seems incompatible with related experimental and theoretical data; this interpretation of the mechanism appears superseded by later work on catalytic conversion. Further experimental work is necessary to help elucidate the reaction mechanism.

In the atmosphere, the high concentrations of H_2O and $(H_2O)_2$ should catalyze the conversion of fluorinated glycolaldehyde to perfluoro glyoxal. Under these conditions, based on the current understanding of the available data, we thus propose that the main observable end products of the OH-

initiated oxidation of perfluorinated methyl vinyl ether are ~60% of perfluoro methyl formate, ~40 % of glyoxal, and a 100% yield of the coproduct CF_2O. A recent experimental and theoretical study on the OH-initiated oxidation of perfluoro propyl vinyl ether (PPVE), $C_3F_7OCF=CF_2$, concluded[11] that the main products of the reaction would be perfluoro propyl formate, C_3F_7OCFO, and CF_2O, with fluorinated glycolaldehyde, $CFOCF_2OH$, as a coproduct. In view of the current analysis, we propose that under atmospheric conditions, the PPVE + OH reaction likewise yields glyoxal, after water-catalyzed decomposition of the fluorinated glycolaldehyde product.

Supporting information

Figures showing all unimolecular reaction channels of the OH adducts ; quantum chemical characteristics of reactants, products, and TS at the M06-2X/cc-pVDZ and M06-2X/aug-cc-pVTZ levels of theory, and various CCSD(T) single point energy calculations.

Acknowledgments

References

1. M. Molina and F. Rowland, *Nature*, 1974, **249**, 810–812.
2. J. C. Farman, B. G. Gardiner, and J. D. Shanklin, *Nature*, 1985, **315**, 207–210.
3. T. J. Wallington, W. F. Schneider, D. R. Worsnop, O. J. Nielsen, J. Sehested, W. J. Debruyn, and J. A. Shorter, *Environ. Sci. Technol.*, 1994, **28**, A320–A326.
4. R. E. Banks, B. E. Smart, and J. C. Tatlow, *Organofluorine chemistry: principles and commercial applications*, 1994.
5. T. Hiyama, *Organofluorine compounds: chemistry and applications*, Springer, Berlin; New York, 2000.
6. Y. Morikawa, W. Chen, T. Hayashi, and T. Uchida, *Jpn. J. Appl. Phys.*, 2003, **42**, 1429–1434.
7. Y. Kondo, K. Ishikawa, T. Hayashi, Y. Miyawaki, K. Takeda, H. Kondo, M. Sekine, and M. Hori, *Jpn. J. Appl. Phys.*, 2015, **54**, 040301.
8. M. Mashino, M. Kawasaki, T. J. Wallington, and M. D. Hurley, *J. Phys. Chem. A*, 2000, **104**, 2925–2930.
9. Z. J. Li, Z. N. Tao, V. Naik, D. A. Good, J. C. Hansen, G. R. Jeong, J. S. Francisco, A. K. Jain, and D. J. Wuebbles, *J. Geophys. Res.-Atmospheres*, 2000, **105**, 4019–4029.
10. K. Tokuhashi, A. Takahashi, M. Kaise, S. Kondo, A. Sekiya, and E. Fujimoto, *Chem. Phys. Lett.*, 2000,

325, 189–195.

11. D. Amedro, L. Vereecken, and J. N. Crowley, *Phys. Chem. Chem. Phys.*, 2015, **17**, 18558–18566.
12. Y. Zhao and D. G. Truhlar, *Theor. Chem. Acc.*, 2008, **120**, 215–241.
13. T. H. Dunning, *J. Chem. Phys.*, 1989, **90**, 1007–1023.
14. I. M. Alecu, J. Zheng, Y. Zhao, and D. G. Truhlar, *J. Chem. Theory Comput.*, 2010, **6**, 2872–2887.
15. J. Zheng, I. M. Alecu, B. J. Lynch, Y. Zhao, and D. G. Truhlar, .
16. D. Jacquemin, E. A. Perpete, I. Ciofini, C. Adamo, R. Valero, Y. Zhao, and D. G. Truhlar, *J. Chem. Theory Comput.*, 2010, **6**, 2071–2085.
17. L. Goerigk and S. Grimme, *Phys. Chem. Chem. Phys.*, 2011, **13**, 6670–6688.
18. M. J. Frisch, G. W. Trucks, H. B. Schlegel, G. E. Scuseria, M. A. Robb, J. R. Cheeseman, G. Scalmani, V. Barone, B. Mennucci, G. A. Petersson, H. Nakatsuji, M. Caricato, X. Li, H. P. Hratchian, A. F. Izmaylov, J. Bloino, G. Zheng, J. L. Sonnenberg, M. Hada, M. Ehara, K. Toyota, R. Fukuda, J. Hasegawa, M. Ishida, T. Nakajima, Y. Honda, O. Kitao, H. Nakai, T. Vreven, J. A. Montgomery Jr., J. E. Peralta, F. Ogliaro, M. Bearpark, J. J. Heyd, E. Brothers, K. N. Kudin, V. N. Staroverov, T. Keith, R. Kobayashi, J. Normand, J. Normand, K. Raghavachari, A. Rendell, J. C. Burant, S. S. Iyengar, J. Tomasi, M. Cossi, N. Rega, J. M. Millam, M. Klene, J. E. Knox, J. B. Cross, V. Bakken, C. Adamo, J. Jaramillo, R. Gomperts, R. E. Stratmann, O. Yazyev, A. J. Austin, R. Cammi, C. Pomelli, J. W. Ochterski, R. L. Martin, K. Morokuma, V. G. Zakrzewski, G. A. Voth, P. Salvador, J. J. Dannenberg, S. Dapprich, A. D. Daniels, O. Farkas, J. B. Foresman, J. V. Ortiz, J. Cioslowski, D. J. Fox, and J. A. Pople, *Gaussian 09, Revision B.01*, Gaussian Inc., Wallington CT, 2010.
19. L. Vereecken, G. Huyberechts, and J. Peeters, *J. Chem. Phys.*, 1997, **106**, 6564–6573.
20. J. R. Barker and C. N. Shovlin, *Chem. Phys. Lett.*, 2004, **383**, 203–207.
21. J. Troe, *J. Chem. Phys.*, 1977, **66**, 4758–4775.
22. J. E. Kilpatrick and K. S. Pitzer, *J. Chem. Phys.*, 1949, **17**, 1064–1075.
23. K. Brudnik, D. Wojcik-Pastuszka, J. T. Jodkowski, and J. Leszczynski, *J. Mol. Model.*, 2008, **14**, 1159–1172.
24. M. T. Nguyen, M. H. Matus, V. T. Ngan, R. Haiges, K. O. Christe, and D. A. Dixon, *J. Phys. Chem. A*, 2008, **112**, 1298–1312.
25. R. J. Buszek and J. S. Francisco, *J. Phys. Chem. A*, 2009, **113**, 5333–5337.
26. B. Long, X. Tan, D. Ren, and W. Zhang, *Chem. Phys. Lett.*, 2010, **492**, 214–219.
27. B. Long, X. Tan, D. Ren, and W. Zhang, *J. Mol. Struct. THEOCHEM*, 2010, **956**, 44–49.
28. K. Brudnik, J. T. Jodkowski, D. Sarzynski, and A. Nowek, *J. Mol. Model.*, 2011, **17**, 2395–2409.
29. N. R. Jensen, D. R. Hanson, and C. J. Howard, *J. Phys. Chem.*, 1994, **98**, 8574–8579.
30. A. A. Turnipseed, S. B. Barone, N. R. Jensen, D. R. Hanson, C. J. Howard, and A. R. Ravishankara, *J. Phys. Chem.*, 1995, **99**, 6000–6009.
31. T. J. Wallington and J. C. Ball, *J. Phys. Chem.*, 1995, **99**, 3201–3205.
32. C. Kelly, H. W. Sidebottom, J. Treacy, and O. J. Nielsen, *Chem. Phys. Lett.*, 1994, **218**, 29–33.
33. J. Calvert, A. Mellouki, J. Orlando, M. Pilling, and T. Wallington, *Mechanisms of Atmospheric Oxidation of the Oxygenates*, Oxford University Press, USA, 2011.
34. V. Saheb and N. Y. Pourhaghighi, *J. Phys. Chem. A*, 2014, **118**, 9941–9950.
35. L. Ai, X. Duan, and J. Liu, *Comput. Theor. Chem.*, 2013, **1013**, 15–22.
36. L. Ai and J. Liu, *J. Mol. Model.*, 2014, **20**, 2179.
37. M. Balaganesh and B. Rajakumar, *J. Mol. Graph. Model.*, 2014, **48**, 60–69.
38. T. J. Wallington, P. Dagaut, and M. J. Kurylo, *Chem. Rev.*, 1992, **92**, 667–710.
39. L. Vereecken and J. Peeters, *Phys. Chem. Chem. Phys.*, 2009, **11**, 9062–9074.
40. R. Atkinson, *Atmos. Environ.*, 2007, **41**, 8468–8485.
41. A. Mellouki, G. Le Bras, and H. Sidebottom, *Chem. Rev.*, 2003, **103**, 5077–5096.

42. M. Mashino, Y. Ninomiya, M. Kawasaki, T. J. Wallington, and M. D. Hurley, *J. Phys. Chem. A*, 2000, **104**, 7255–7260.
43. T. J. Wallington, M. P. S. Andersen, and O. J. Nielsen, *Atmos. Environ.*, 2010, **44**, 1478–1481.
44. B. Du, C. Feng, and W. Zhang, *Chem. Phys. Lett.*, 2009, **479**, 37–42.
45. B. Long, X. Tan, Z. Long, D. Ren, and W. Zhang, *Chin. J. Chem. Phys.*, 2011, **24**, 16–21.
46. J. Sehested and T. J. Wallington, *Environ. Sci. Technol.*, 1993, **27**, 146–152.
47. T. J. Wallington and W. F. Schneider, *Environ. Sci. Technol.*, 1994, **28**, 1198–1200.
48. W. F. Schneider, T. J. Wallington, K. Minschwaner, and E. A. Stahlberg, *Environ. Sci. Technol.*, 1995, **29**, 247–250.
49. L. G. Huey, D. R. Hanson, and E. R. Lovejoy, *J. Geophys. Res.-Atmospheres*, 1995, **100**, 18771–18774.
50. G. Bednarek, J. P. Kohlmann, H. Saathoff, and R. Zellner, *Z. Für Phys. Chem.*, 1995, **188**, 1–15.
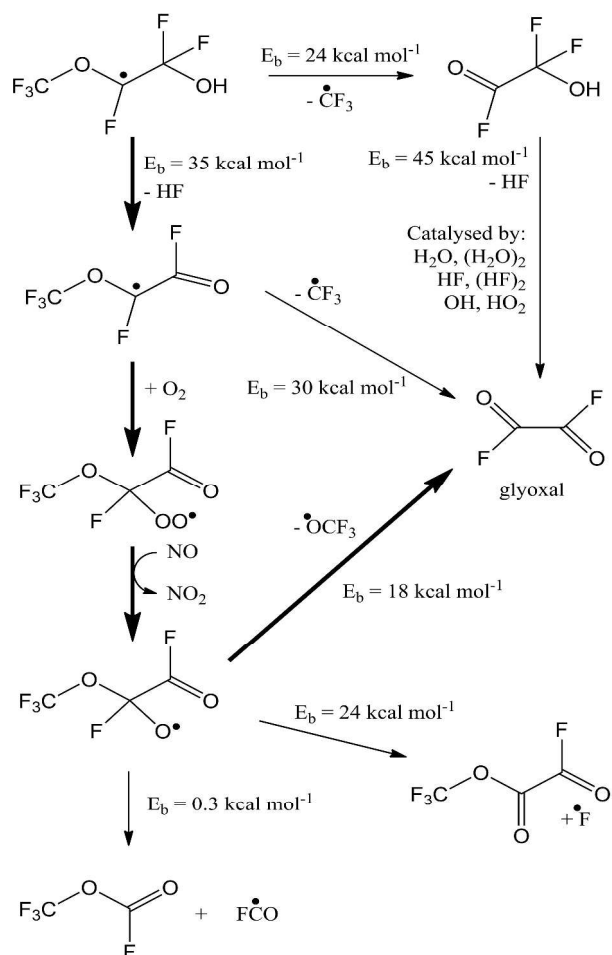51. A. I. Alrawashdeh and R. A. Poirier, *J. Phys. Chem. A*, 2015, **119**, 3615–3620.

Figure 1: Pathways potentially forming perfluoro glyoxal from the main adduct, characterized at the M06-2X/aug-cc-pVTZ level of theory. Bold arrows show the HF loss and subsequent glyoxal formation route proposed by Li et al.[9] and Mashino et al.[8]

Figure 2 : Most relevant pathways for the main adduct in the reaction of PVME + OH, as calculated at the M06-2X/aug-cc-pVTZ level of theory. See supporting information for additional pathways.
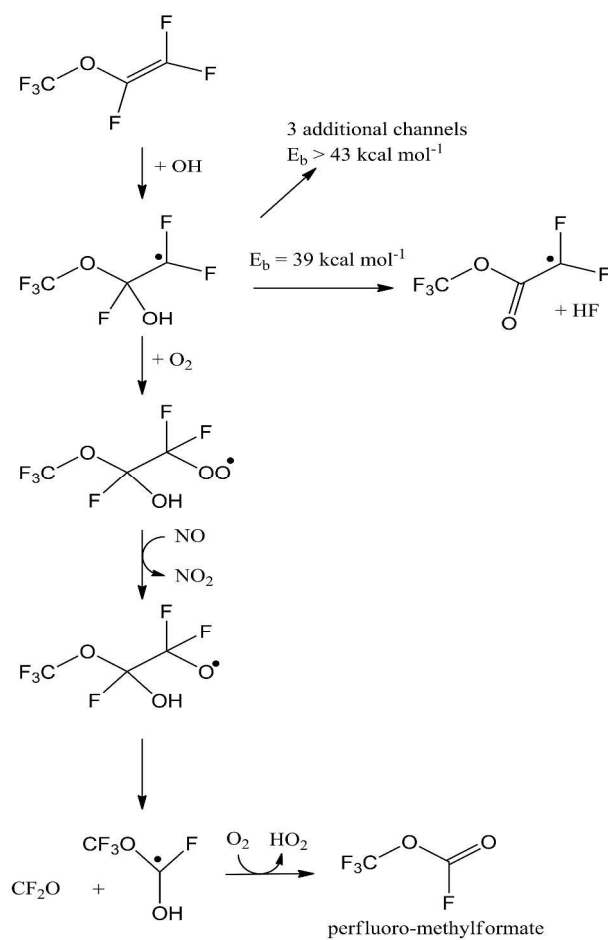
Figure 3 : Dominant pathways for the degradation of the minor adduct, at the M06-2X/aug-cc-pVTZ level of theory. See supporting information for additional pathways.